Spin alignment and density matrix measurement in $^{28}Si + ^{12}C$ orbiting reaction

A. Ray
Joint Institute for Heavy Ion Research, Oak Ridge National Laboratory, Oak Ridge, Tennessee 37831

D. Shapira, M. L. Halbert, J. Gomez del Campo, and H. J. Kim
Oak Ridge National Laboratory, Oak Ridge, Tennessee 37831

J. P. Sullivan
Cyclotron Institute, Texas A&M University, College Station, Texas 77843

B. Shivakumar and J. Mitchell
Wright Nuclear Structure Laboratory, Yale University, New Haven, Connecticut 06511
(Received 19 July 1990)

Gamma-ray angular correlations have been measured for the damped reactions $^{12}C(^{28}Si,^{12}C)^{28}Si$ between $\theta_{c.m.}=120°$ and 160° for $E_{c.m.}=43.5$ and 48 MeV. The spin alignments and density matrices have been deduced from the observed angular distribution of the gamma rays for ^{28}Si states in $-10<Q<0$ and $-16<Q<0$ MeV for $E_{c.m.}=43.5$ and 48 MeV, respectively, and for $^{12}C(2_1^+)$ state in strongly damped region $Q<-10$ MeV. We find that the spin angular momenta of the nuclei are poorly aligned with respect to the normal to the reaction plane and the density matrices for the $^{12}C(2_1^+)$ and ^{28}Si states are almost diagonal with respect to the direction of motion of the outgoing particle. We also find qualitatively similar behavior of the spin alignments for ^{28}Si states in strongly damped region. The measured density matrices and spin alignments are consistent with the picture of formation of a long-lived dinuclear complex undergoing orbiting, bending, and wriggling motions, but not with those obtained from statistical compound nucleus or sticking-model calculations.

I. INTRODUCTION

It has been suggested[1,2,3] that damped reaction products at backward angles from the $^{28}Si+^{12}C$ (Ref. 1), $^{20}Ne+^{12}C$ (Ref. 2), and $^{16}O + ^{27}Al$ (Ref. 3), reactions result from the formation of long-lived orbiting complexes. This suggestion was originally made on the basis of the observations that the total integrated damped binary yields are much larger compared to the predictions of compound nucleus calculations and follow a $1/\sin\theta_{c.m.}$ angular distribution near 180°. It was suggested that the two nuclei instead of fusing form a dinuclear intermediate state in which they maintain their identities and then break apart producing a large yield in the entrance channel compared to statistical model calculations. A constrained phase-space model with a dinuclear sticking-model configuration has been developed by Shivakumar *et al.*[4] This model, usually referred to as the equilibrated orbiting model, successfully explains the observed large, damped binary yields in several cases such as $^{28}Si+^{12}C$ (Ref. 4), and $^{28}Si+^{14}N$ (Ref. 5). Measurements of the $^{32}S+^{24}Mg$ (Ref. 6) and $^{35}Cl+^{12}C$ (Ref. 7) systems show smaller yields of ^{12}C and similar products. The analysis[6,7] suggests that asymmetric fission is more successful than the equilibrated orbiting model in accounting for the yields of ^{12}C and similar products. There has been a controversy[6-8] in the literature regarding these two models. Both models are statistical. The controversy is mainly focused on the calculation of absolute yields of damped ^{12}C and similar products. The statistical model calculation for the yield of these heavy fragments is sensitive to the level density parameter and to the optical model parameters used to calculate transmission coefficients, critical angular momentum and spin distribution of the compound nucleus. However, despite the uncertainties in compound nucleus calculations, it is clear that the compound nucleus yield is dominant in some systems such as $^{32}S+^{24}Mg$ and $^{35}Cl+^{12}C$, but orbiting yield is dominant in some other systems, such as $^{28}Si+^{12}C$, $^{24}Mg+^{16}O$, etc., because of observed very large yield in these systems.

It should also be noted that the equilibrated orbiting model does not incorporate the shape degree of freedom of the two nuclei and the dinuclear dynamics of the intermediate state. The main difference between the orbiting picture and the statistical model is the assumption that, in the orbiting picture, the reaction goes via a dinuclear intermediate state rather than a compound nucleus. In the orbiting picture, the shape degree of freedom never equilibrates and the dinuclear dynamics of the intermediate state could be important. The equilibrated orbiting model considers an orbiting picture assuming statistical equilibrium. So, the equilibrated orbiting model fails to explain several important nonstatistical features of the orbiting reaction, which differentiates this reaction from the compound nucleus reaction.

The most important criteria of orbiting reaction are the entrance-channel effects[9] as observed in $^{28}Si+^{12}C$ versus $^{24}Mg+^{16}O$ reactions, very large yield and selective population[10] of natural parity states as observed in the $^{24}Mg+^{12}C$ reaction. The observation of entrance-channel effects in the orbiting reaction cannot be explained by any statistical model, including the equilibrated orbiting model, and suggests that the shape degree of freedom never equilibrates in these reactions. These observations point to the nonstatistical features associated with the orbiting reaction. We also find that in systems where orbiting has been seen, all the important criteria[9,10] of orbiting reaction have been observed within reasonably damped region $-15<Q<0$ MeV. The orbiting reaction cannot be characterized by Q-value or l-value windows only and the reasons for observing orbiting in some light heavy ion systems and not in others have not been fully understood yet.

The gamma-ray angular correlation measurements in orbiting reaction can also provide important information about the reaction mechanism. The population of magnetic substates of $^{12}C(2_1^+)$ and ^{28}Si states for the $^{12}C(^{28}Si,^{12}C)^{28}Si$ orbiting reaction at $\theta_{c.m.}=180°$ has been measured.[11] The observed selective population[11] of the $m=0$ magnetic substate with respect to the beam axis agrees qualitatively with a simple dinuclear sticking model.[1,11] On the other hand, according to this model[1,11] both of the nuclei should generally come out in excited states, but the data show that most of the time ^{12}C comes out in its ground state (70%) and the entire excitation energy goes to ^{28}Si. The observed division of excitation energy can be obtained from a constrained phase-space calculation[11] which assumes that only the $m=0$ magnetic substate with respect to the beam axis is excited. Although a constrained phase-space model with the dinuclear sticking-model configuration is adequate to explain the observed γ-ray angular correlation at $\theta_{c.m.}=180°$, no test has been made of whether this model can reproduce the γ-ray angular correlation at different angles. One expects complete alignment of fragment spins with respect to the normal to the scattering plane on the basis of the simple sticking model. From statistical model calculations, one also expects large alignment of fragment spins with respect to the normal to the scattering plane and the spin orientation of the emitted fragments should be approximately cylindrically symmetric with respect to the normal to the reaction plane.

In this paper, we report a new particle–γ-ray coincidence measurement and discuss how the structure of the orbiting complex influences the density matrices and spin alignment parameters of $^{12}C(2_1^+)$ and ^{28}Si states as a function of emission angle.

II. EXPERIMENTAL PROCEDURE

In this experiment, we studied the $^{28}Si+^{12}C$ system at $E_{c.m.}=43.5$ and 48 MeV using reverse kinematics. Natural carbon foils (150 $\mu g/cm^2$) were bombarded by 8 pna of ^{28}Si beam from the HHIRF tandem accelerator at $E_{lab}=145$ and 160 MeV. The carbon foil was placed at the center of a cryogenically pumped spherical chamber of 17.78 cm radius. Three ΔE-E silicon detector telescopes were placed in a horizontal plane at $\theta_{lab}=10°$, 15°, and 25° with circular apertures subtending half angles of 1.3°, 1.6°, and 2°, respectively. The thicknesses of the ΔE surface barrier detectors placed at 10°, 15°, 25° and 54.2, 52.3, 47.4 μm, respectively. The E detectors were about 500 μm thick. These telescopes were used to identify carbon particles using energy and energy loss signals. The thresholds of the ΔE detectors were raised high enough to cut off all light particles including α particles.

The experiment was performed in the Oak Ridge National Laboratory Spin Spectrometer.[12] The chamber was surrounded by 70 NaI detectors covering 94% of the total solid angle. A lead plate about 0.64 cm thick was placed in front of each NaI detector to absorb low-energy γ rays. We recorded event by event NaI energy signals, timing signals between each NaI and each silicon E detector, energy (E) and energy loss (ΔE) signals. Our count rate was limited by the singles rate of the NaI detectors and that of the most-forward-angle (10°) ΔE detector. The count rates for the backward-angle NaI detectors were about 23 kHz and those for the most-forward-angle NaI detectors were about 55–60 kHz. The ΔE solid-state detector placed at 10° had a singles count rate of about 1 kHz. The relative efficiencies of the NaI detectors as a function of energy were obtained by measurements with γ-ray sources. Absolute efficiencies at 4.44 MeV were obtained by bombardment of a carbon target of known thickness with a 17 MeV proton beam for a measured total number of protons, together with the known differential γ-ray cross section[13] for production of 4.44 MeV γ rays.

III. DATA ANALYSIS AND EXPERIMENTAL RESULTS

Figure 1 shows a typical ΔE-E spectrum for the telescope at $\theta_{lab}=10°$. We can clearly identify the carbon band from this spectrum. Figure 2 shows a typical time spectrum in coincidence with the carbon particles. The random coincidence background is small and the contributions from the low-energy neutrons emitted by excited ^{28}Si are negligible. Figure 3 shows a singles carbon-particle energy spectrum obtained at $\theta_{lab}=10°$ at $E_{lab}=145$ MeV. We gated on three different Q-value bins $-10<Q<0$, $-22<Q<-10$, and $-40<Q<-22$ MeV of the carbon band and corresponding time spectrum between 140 and 185 ns and obtained the pulse-height spectrum of each of the 70 NaI detectors in coincidence with carbon particles detected at each particle telescope. In order to improve the γ-ray peak-to-background ratio, we performed cluster summing of the NaI detectors. That is, for each event, the NaI crystal that received the maximum energy was identified and its pulse height was summed with those in all the adjacent crystals. Then the second maximum pulse height was searched for and again the energy deposited in the adjacent crystals were added to the maximum. We looked for five such clusters in each event, because the γ multiplicity is not more than five in the reaction being studied. We also subtracted out the random coincidence background from each NaI spectrum. The background subtraction was less than 5% in

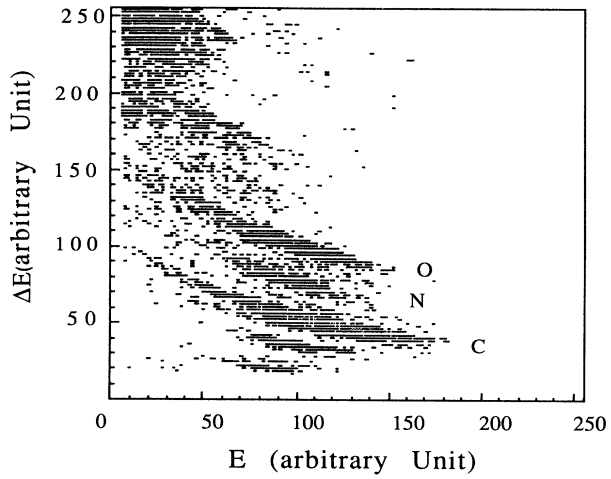

FIG. 1. A typical two-dimensional spectrum of energy versus energy loss in ΔE-E telescope detector placed at $\theta_{lab}=10°$.

all cases.

Let us discuss the observed γ-ray and particle spectra. Figures 4–6 show examples of NaI spectra in coincidence with carbon particles detected at $\theta_{lab}=15°$ at $E_{c.m.}=43.5$ MeV for $-10<Q<0$, $-22<Q<-10$, and $-40<Q<-22$ MeV, respectively. At all angles we observe Doppler-shifted 1.78 and 2.84 MeV γ-ray lines from the 2^+-0^+ and 4^+-2^+ transitions in ^{28}Si, 1.34 MeV γ rays from 2^+-0^+ transitions in ^{24}Mg and 4.44 MeV γ rays from ^{12}C (2^+-O^+) transitions. The spectra show a peak corresponding to decay of the first excited state of ^{24}Mg (1.34 MeV). This peak becomes visible at high excitation energies, and presumably arises from the cooling down of ^{24}Mg formed from unbound ^{28}Si. The large Doppler shift of the 4.44 MeV γ rays indicates that they are mostly coming from the 2^+-0^+ transition in the fast moving ^{12}C. The observations of comparable yields at $\theta=174°$, 88°, 102.3° for both 4.44 and 1.78 MeV γ rays imply rather poor spin alignments for both ^{12}C(2^+) and ^{28}Si(2^+) states, in disagreement with the simple dinuclear sticking model[1,11] for which the expectation would be

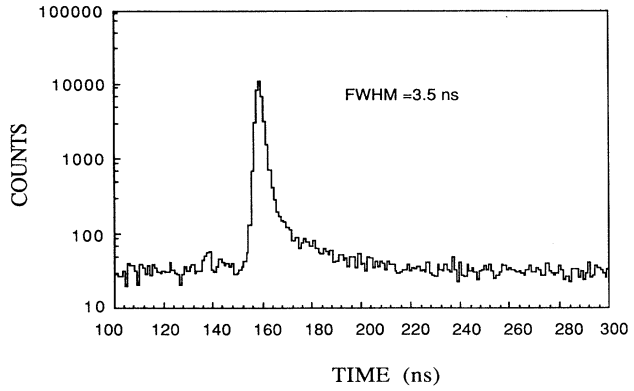

FIG. 2. A typical coincidence time spectrum between E detector at $\theta_{lab}=10°$ and a NaI detector.

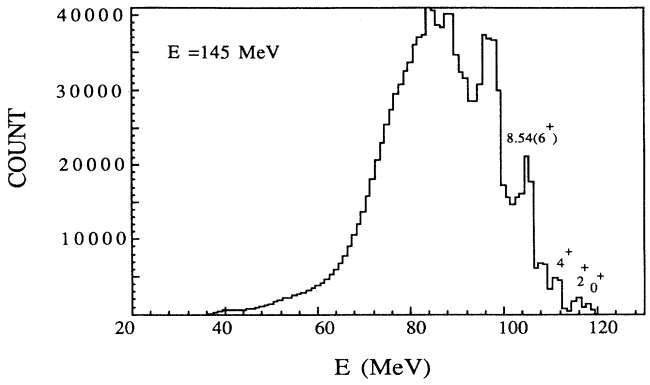

FIG. 3. Singles carbon energy spectrum at $\theta_{lab}=10°$ at $E_{lab}=145$ MeV.

that the yield at $\theta=88°$ should be a factor of 7 larger than the yield at $\theta=174°$. Figure 7 shows a singles carbon-particle energy spectrum obtained at $\theta_{lab}=10°$ at $E_{lab}=160$ MeV. We gated on three different Q-value bins $-16<Q<0$, $-26<Q<-16$, $-44<Q<-26$ MeV of the carbon band and performed similar analyses. Figures 8–10 show examples of NaI spectra in coincidence with carbon particles detected at $\theta_{lab}=15°$ at $E_{c.m.}=48$ MeV for $-16<Q<0$, $-26<Q<-16$, $-44<Q<-26$ MeV, respectively. We make similar observations of poor spin alignment for ^{12}C(2^+) and ^{28}Si(2^+) states at $E_{lab}=160$ MeV also.

A complete study of the γ-ray angular correlation has been done. The γ-ray angular correlation function can be written as[14]

$$W(\theta,\phi)=\sum_k \sum_q [4\pi/(2k+1)]^{1/2} t_{kq}(J) R_k Y_{kq}(\theta,\phi) , \quad (1)$$

where θ, ϕ are polar and azimuthal angles of the direction of emission of the γ rays, Y_{kq} is the spherical harmonic function, R_k is the radiation parameter, t_{kq} is the

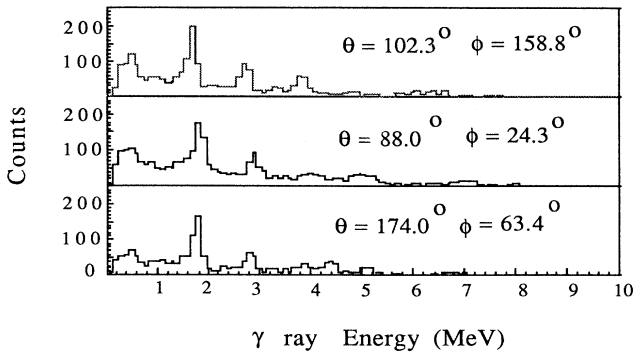

FIG. 4. Coincidence NaI spectra for the reaction ^{28}Si+^{12}C at $E_{c.m.}=43.5$ MeV and $-10<Q<0$ MeV at $\theta_{lab}=15°$, $\phi_{lab}=0°$. Polar and azimuthal angles are measured in a coordinate frame whose Z axis is normal to the reaction plane and X axis is along the beam direction.

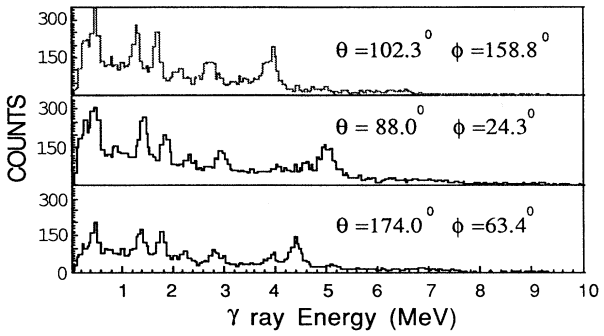

FIG. 5. Coincidence NaI spectra for the reaction $^{28}Si+^{12}C$ at $E_{c.m.}=43.5$ MeV and $-22<Q<-10$ MeV at $\theta_{lab}=15°$, $\phi_{lab}=0°$. Polar and azimuthal angles are measured in a coordinate frame whose Z axis is normal to the reaction plane and X axis is along the beam direction.

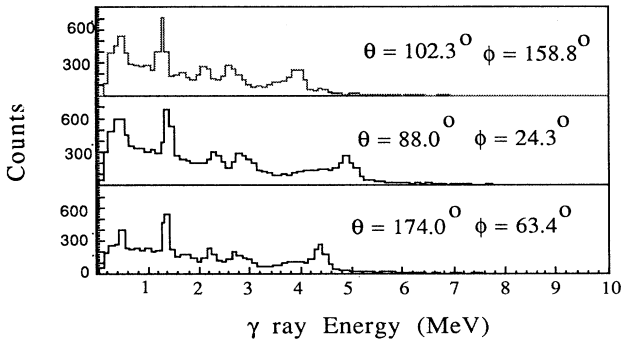

FIG. 6. Coincidence NaI spectra for the reaction $^{28}Si+^{12}C$ at $E_{c.m.}=43.5$ MeV and $-40<Q<-22$ MeV at $\theta_{lab}=15°$, $\phi_{lab}=0°$. Polar and azimuthal angles are measured in a coordinate frame whose Z axis is normal to the reaction plane and X axis is along the beam direction.

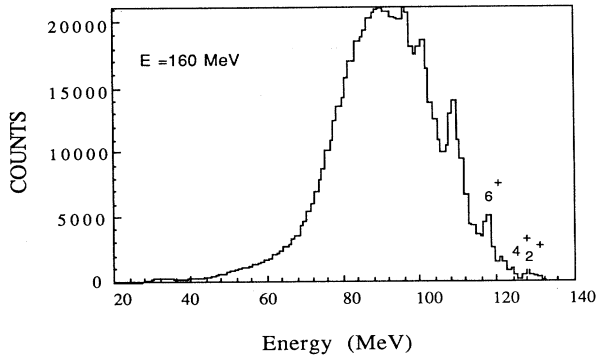

FIG. 7. Singles carbon energy spectrum at $\theta_{lab}=10°$ at $E_{lab}=160$ MeV.

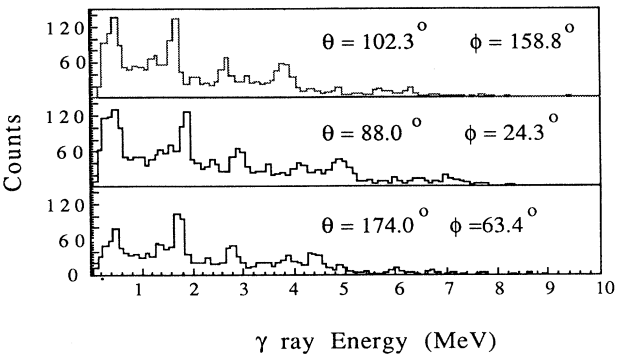

FIG. 8. Coincidence NaI spectra for the reaction $^{28}Si+^{12}C$ at $E_{c.m.}=48.0$ MeV and $-16<Q<0$ MeV at $\theta_{lab}=15°$, $\phi_{lab}=0°$. Polar and azimuthal angles are measured in a coordinate frame whose Z axis is normal to the reaction plane and X axis is along the beam direction.

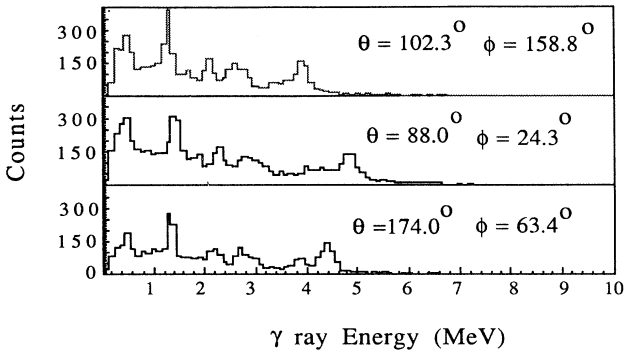

FIG. 9. Coincidence NaI spectra for the reaction $^{28}Si+^{12}C$ at $E_{c.m.}=48.0$ MeV and $-26<Q<-16$ MeV at $\theta_{lab}=15°$, $\phi_{lab}=0°$. Polar and azimuthal angles are measured in a coordinate frame whose Z axis is normal to the reaction plane and X axis is along the beam direction.

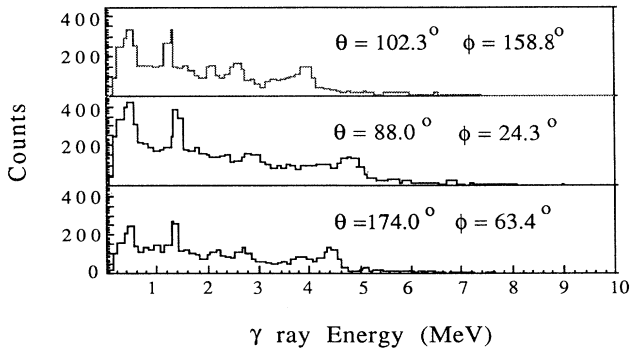

FIG. 10. Coincidence NaI spectra for the reaction $^{28}Si+^{12}C$ at $E_{c.m.}=48.0$ MeV and $-44<Q<-26$ MeV at $\theta_{lab}=15°$, $\phi_{lab}=0°$. Polar and azimuthal angles are measured in a coordinate frame whose Z axis is normal to the reaction plane and X axis is along the beam direction.

polarization tensor, and J is the spin of the emitting nucleus. We obtain values of the radiation parameter R_k from the tabulations in Ref. 15. We now choose a coordinate frame whose Z axis is along the direction of motion of the nucleus emitting γ rays and whose Y axis is normal to the reaction plane and consider γ-ray emission from the 2^+-0^+ transition. Then considering[14] symmetry properties of the polarization tensor and the conservation of parity we find nine independent elements of the polarization tensor $(t_{00}, t_{20}, t_{21}, t_{22}, t_{40}, t_{41}, t_{42}, t_{43}, t_{44})$. These elements must be real numbers.[14] The elements of the density matrix ρ are given by the expression[14]

$$\rho_{mm'} = \sum_k \sum_q t_{kq}(J)\langle J, J, m', -m/k, q\rangle(-1)^{J-m} . \quad (2)$$

We used the 4.44 and 1.78 MeV γ-ray yields from the NaI detectors of the Spin Spectrometer to determine the nine elements of each of the corresponding polarization tensors by fitting them with Eq. (1), after taking into account the finite solid angle of the NaI detectors and the Doppler shifts. The energy resolution was poor in ten of the NaI detectors, so only 60 NaI detectors were used in our analysis. The attenuation[16] due to the hyperfine interaction has been estimated to be (2–3)% and we did not correct for it. Subsequently, the elements of the density matrices of $^{12}C(2^+)$ and $^{28}Si(2^+)$ states were determined by using Eq. (2). Then the matrices were rotated to a coordinate frame whose Z axis is along the normal to the reaction plane defined by the beam axis and the direction of motion of the scattered carbon particle. The spin alignment parameter with respect to the Z axis is defined[17] as

$$P_{zz} = \frac{3\sum_m m^2 \rho_{mm} - J(J+1)}{J(2J-1)} .$$

The spin alignment parameter is conserved for stretched $E2$ transitions. Particle emission and nonstretched transitions tend to decrease P_{zz}. In $-10 < Q < 0$ MeV, ^{28}Si is predominantly (90%) excited to 6^+, 4^+, and 2^+ states as shown in Fig. 3. These states decay by stretched $E2$ cascades that preserve the alignment. So in $-10 < Q < 0$ MeV, the spin alignments of the $^{28}Si(2^+)$ state as obtained from the angular distribution of 1.78 MeV γ rays and those of the original parent states of ^{28}Si should be about the same. We measured the angular distribution of 4.44 MeV γ rays to determine the spin alignment and density matrices of the $^{12}C(2^+)$ state. All states of ^{12}C above 4.44 MeV are particle unbound and decay predominantly by particle emission. We find by use of CASCADE statistical model[18] calculation that the ratio of cross sections for populating the ^{12}C(7.564 MeV) and the ^{12}C(4.44 MeV) state is only 3% for the reactions being studied, and the probability of populating higher-lying states in ^{12}C is even smaller. However, the $^{12}C(2^+)$ state might be excited by the following sequential decay:

$$^{28}Si + ^{12}C \rightarrow ^{24}Mg^* + ^{16}O^* \rightarrow ^{24}Mg^* + ^{12}C(2^+) + ^4He ,$$

if the ^{16}O is excited to at least 16–17 MeV. In the $-22 < Q < -10$ MeV region, such a process is very unlikely to happen according to the CASCADE model calculations and present and previous[11] measurements. In Fig. 11, we show P_{zz} (Z axis normal to the reaction plane) of the $^{12}C(2^+)$ state in $-22 < Q < -10$ MeV and the $^{28}Si(2^+)$ state in $-10 < Q < 0$ MeV as a function of emission angle of the carbon particle at $E_{c.m.} = 43.5$ MeV. In Fig. 12, we show P_{zz} for $^{12}C(2^+)$ and $^{28}Si(2^+)$ states in $-16 < Q < 0$ and $-26 < Q < -16$ MeV as a function of emission angle of the carbon particle at $E_{c.m.} = 48$ MeV. The values and variations of P_{zz} as a function of emission angle are similar for the two bombarding energies. Error estimates were obtained by adding in quadrature the error in determining the area under the peak and the error in the relative gamma detector efficiencies. As a check, we also determined the magnetic substate population ρ_{11} of the $^{28}Si(2^+)$ state for $-3 < Q < -0.6$ MeV using a coordinate system whose Z axis is normal to the reaction plane. We find that ρ_{11} is consistent with zero within the statistical uncertainties, as required by the conservation of parity and rotational invariance. We also obtained small spin alignments (0.15) for $^{28}Si(2^+)$ and $^{24}Mg(2^+)$ states for $Q < -15$ MeV. However it is difficult to interpret the spin alignment of the original parent state in these Q-value bins because of nonstretched transitions and particle emissions. In Fig. 13, we show that the values of P_{zz} for $^{12}C(2^+)$ drop to about 0.1 ± 0.05 for $-40 < Q < -22$ and $-44 < Q < -26$ MeV for both bombarding energies.

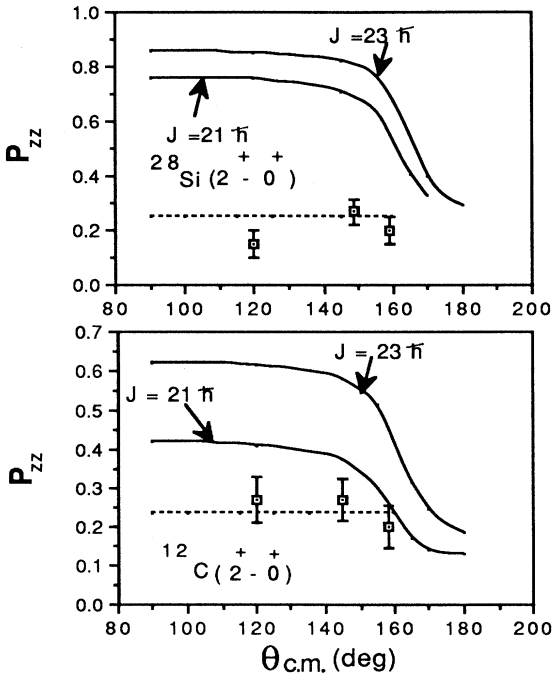

FIG. 11. The spin alignment parameter of 1.78 MeV γ rays for $-10 < Q < 0$ MeV and of 4.44 MeV γ rays for $-22 < Q - 10$ MeV at $E_{c.m.} = 43.5$ MeV. The solid curves and dashed lines are statistical and dinuclear orbiting model calculations, respectively, as explained in the text.

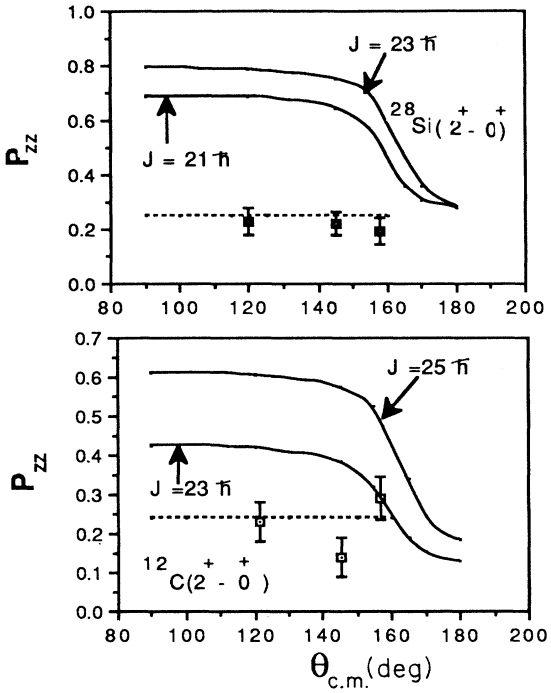

FIG. 12. The spin alignment parameter of 1.78 MeV γ rays for $-16<Q<0$ MeV and of 4.44 MeV γ rays for $-26<Q-16$ MeV at $E_{\text{c.m.}}=48.0$ MeV. The solid curves and dashed lines are statistical and dinuclear orbiting model calculations, respectively, as explained in the text.

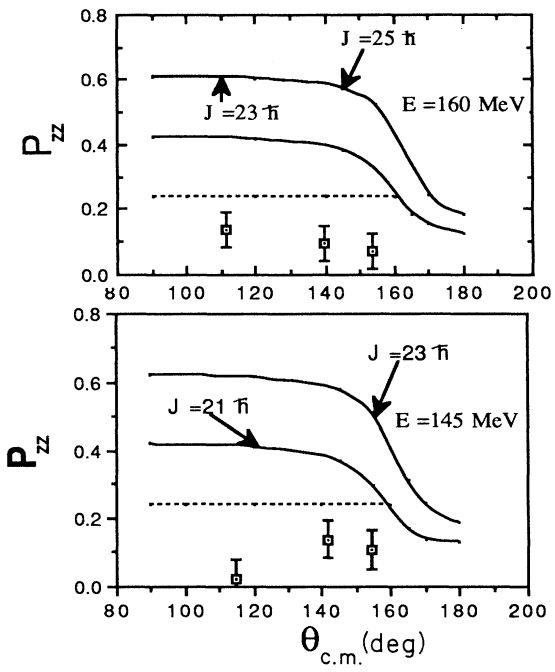

FIG. 13. The spin alignment parameter of 4.44 MeV $^{12}C(2^+\text{-}O^+)$ γ rays for $-40<Q<-22$ MeV at $E_{\text{c.m.}}=43.5$ MeV and 4.44 MeV $^{12}C(2^+\text{-}O^+)$ γ rays for $-44<Q-26$ MeV at $E_{\text{c.m.}}=48.0$ MeV. The solid curves and dashed lines are statistical and dinuclear orbiting model calculations, respectively, as explained in the text.

We now discuss the off-diagonal elements of the density matrices. For this purpose, we choose a coordinate frame whose Z axis is along the direction of the nucleus emitting γ rays and whose Y axis is normal to the reaction plane. Let Z_{Si} and Z_{C} denote the directions of motion of ^{28}Si and ^{12}C nuclei, respectively. In Table I, we show the deduced density matrix of the ^{12}C (2^+) state for $\theta_{\text{c.m.}}=145°$ in the range $-22<Q<-10$ MeV at $E_{\text{c.m.}}=43.5$ MeV. We find that the density matrix is almost diagonal with respect to the direction of motion of the particle. This means that the spin orientation of the $^{12}C(2^+)$ state is cylindrically symmetric with respect to its direction. Table I also shows the density matrix of the $^{28}Si(2^+)$ state for $\theta_{\text{c.m.}}=148°$ in the range $-10<Q<0$ MeV at $E_{\text{c.m.}}=43.5$ MeV. The orientation of the $^{28}Si(2^+)$ state is also found to be approximately cylindrically symmetric with respect to its direction of motion. Since the $^{28}Si(2^+)$ state is mostly populated by stretched $E2$ transitions in the $-10<Q<0$ MeV region, the orientations of the parent ^{28}Si states are also approximately cylindrically symmetric with respect to the direction of motion of the ^{28}Si ion. Similar behavior of the density matrix was

TABLE I. Density matrices for $^{12}C(2_1^+)$ and $^{28}Si(2_1^+)$ states.

Observation $^{12}C(2_1^+)$[a]	$^{28}Si(2_1^+)$ [b]	Statistical model[c] $^{12}C(2_1^+)$	Dinuclear model[d] $^{12}C(2_1^+)$
$\rho_{00}=0.27\pm0.02$	0.29 ± 0.019	0.31	0.29
$\rho_{11}=0.28\pm0.013$	0.23 ± 0.011	0.235	0.24
$\rho_{22}=0.08\pm0.02$	0.13 ± 0.014	0.11	0.11
$\rho_{01}=0.014\pm0.012$	0.005 ± 0.017	0.012	0
$\rho_{02}=-0.019\pm0.011$	-0.028 ± 0.01	-0.102	-0.013
$\rho_{12}=0.018\pm0.013$	-0.027 ± 0.011	0.022	0
$\rho_{1-1}=-0.017\pm0.015$	-0.05 ± 0.01	-0.132	-0.041
$\rho_{1-2}=0.007\pm0.01$	-0.007 ± 0.009	0.0062	0
$\rho_{2-2}=0.004\pm0.012$	0.012 ± 0.011	0.0095	0.0015

[a] Z_{C} as Z axis, $-22<Q<-10$ MeV, $\theta_{\text{c.m.}}=145°$, $E_{\text{c.m.}}=43.5$ MeV.
[b] Z_{Si} as Z axis, $-10<Q<0$ MeV, $\theta_{\text{c.m.}}=148°$, $E_{\text{c.m.}}=43.5$ MeV.
[c] Z_{C} as Z axis, $-22<Q<10$ MeV, $E_{\text{c.m.}}=43.5$ MeV.
[d] Orbiting, bending and wriggling modes, Z_{C} as Z axis.

found at other scattering angles and at the other energy. Table II shows the deduced density matrix of $^{12}C(2^+)$ state for $\theta_{c.m.}=139.2°$ in the range $-40<Q<-22$ MeV at $E_{c.m.}=43.5$ MeV and for $\theta_{c.m.}=138.2°$ in the range $-44<Q<-26$ MeV at $E_{c.m.}=48$ MeV. We still find symmetry around the direction of motion of the carbon particle. However ρ_{22} along the direction of motion of ^{12}C has increased and so the value of the spin alignment parameter has decreased. We obtained the $^{12}C(2^+)$ yield by integrating over the 4.44 MeV γ rays and measuring the efficiency of detecting 4.44 MeV γ rays in the Spin Spectrometer. Table III shows the ratios of yields of $^{12}C(2^+)$ to ^{12}C(g.s.) integrated over $Q<-10$ MeV at $E_{c.m.}=43.5$ MeV and $Q<-15$ MeV at $E_{c.m.}=48$ MeV. Error estimates were obtained by adding in quadrature the error in determining the total number of 4.44 MeV γ rays and the error in determining the absolute efficiency of detecting 4.44 MeV γ rays in the Spin Spectrometer. The error in determining the absolute detection efficiency comes from the uncertainties in determining the target thickness, the total number of incident particles on the target and the uncertainties in the known γ-ray cross section.

TABLE II. Density matrices for $^{12}C(2^+)$ state for large Q-value bins.

Observation		Dinuclear model[c]
$^{12}C(2^+)$[a]	$^{12}C(2^+)$[b]	$^{12}C(2^+)$
$\rho_{00}=0.215\pm0.024$	0.23 ± 0.020	0.29
$\rho_{11}=0.25\pm0.014$	0.22 ± 0.012	0.24
$\rho_{22}=0.14\pm0.02$	0.16 ± 0.015	0.11
$\rho_{01}=-0.005\pm0.013$	-0.007 ± 0.012	0
$\rho_{02}=-0.0025\pm0.011$	-0.005 ± 0.010	-0.013
$\rho_{12}=-0.0011\pm0.013$	-0.0095 ± 0.012	0
$\rho_{1-1}=-0.037\pm0.016$	-0.033 ± 0.014	-0.041
$\rho_{1-2}=0.0051\pm0.0097$	0.023 ± 0.013	0
$\rho_{2-2}=0.027\pm0.016$	0.023 ± 0.0094	0.0015

[a] Z_C as Z axis, $-40<Q<-22$ MeV, $\theta_{c.m.}=139.2°$, $E_{c.m.}=43.5$ MeV.
[b] Z_C as Z axis, $-44<Q<-26$ MeV, $\theta_{c.m.}=138.2°$, $E_{c.m.}=48$ MeV.
[c] Z_C as Z axis.

IV. DISCUSSION AND COMPARISON WITH MODELS

We have measured the spin alignments and density matrices of ^{28}Si and ^{12}C nuclei by measuring the $^{28}Si(2^+\text{-}0^+)$ and $^{12}C(2^+\text{-}0^+)$ transitions in coincidence with carbon particle. We obtain the values of spin alignments around 0.25 for $^{28}Si(2^+)$ state in $-15<Q<0$ MeV and those of around 0.15 for $^{28}Si(2^+)$ and $^{24}Mg(2^+)$ states in strongly damped regions $Q<-15$ MeV. In this reaction, ^{28}Si is initially produced with high spin and large excitation energy and then decays predominantly to $^{28}Si(2^+)$ or $^{24}Mg(2^+)$ states. In strongly damped region $Q<-15$ MeV, we cannot identify, from our carbon spectrum, the individual ^{28}Si states decaying to $^{28}Si(2^+)$ or $^{24}Mg(2^+)$ states and also do not know about their complete decay schemes. The observation of somewhat smaller spin alignments of $^{28}Si(2^+)$ and $^{24}Mg(2^+)$ states in strongly damped regions is most likely the result of particle emission and nonstretched transitions from parent ^{28}Si states. Qualitatively speaking, we do not find any strong variation of spin alignments with Q value. The observation of poor spin alignment in all Q-value regions suggests that similar reaction mechanism is dominant in those Q-value regions. In strongly damped region, we have not determined quantitatively the spin alignments and density matrices of the parent ^{28}Si states from $^{28}Si(2^+\text{-}0^+)$ and $^{24}Mg(2^+\text{-}0^+)$ transitions because of our lack of knowledge of complete decay schemes and identification of the parent states. So we discuss about the spin alignments and density matrices of $^{28}Si(2^+)$ state in $-15<Q<0$ MeV where we can infer about the spin alignments and properties of density matrices of the parent ^{28}Si state from our measurements. We also find from Ref. 9 that for $^{24}Mg+^{16}O$ system, the integrated yield in $-8.5<Q<0$ MeV follows the same $1/\sin\theta_{c.m.}$ angular distribution as the more strongly damped yield does and also there is strong entrance-channel effect in the less damped regions. As we discussed earlier, the main criteria of orbiting reaction are large yield, entrance-channel effect and selection of natural parity states in addition to long life time. All these criteria are satisfied in less damped regions also. We also discuss about the spin alignments and density matrices of $^{12}C(2^+)$ state in strongly damped regions because there is very small probability ($<1\%$) that this state is populated by the decay of excited ^{16}O in the $-30<Q<0$ MeV region and about (30–50)% of the reaction yield goes to $^{12}C(2^+)$ state as shown in Table III. In the following sections, we compare our observations of spin alignments, density matrices and ratios of yields of $^{12}C(2^+)$ to ^{12}C(g.s.) integrated

TABLE III. Ratio of yields of $^{12}C(2^+)$ to ^{12}C(g.s.).

Laboratory energy (MeV)	Laboratory angle (deg)	$^{12}C(2^+)/^{12}C$(g.s.)	Statistical model
145	10	0.56 ± 0.085	
145	15	0.60 ± 0.09	0.944
145	25	0.56 ± 0.085	
160	10	0.94 ± 0.15	
160	15	0.87 ± 0.13	1.24
160	25	0.87 ± 0.13	

over various excitation ranges of ^{28}Si in strongly damped region and those of ^{28}Si states in less damped region with the corresponding predictions of the statistical model, the sticking model, and a simple dinuclear orbiting model.

A. Statistical model

In Figs. 11 and 12, the solid curves are the predictions of a compound-nuclear statistical model. We assume that ^{12}C and ^{28}Si form a compound nucleus and consider emission of ^{12}C from the compound nucleus. Let **J**, $\mathbf{S}_{\mathrm{Si}}$, $\mathbf{S}_{\mathrm{C}}$, **S** and $\boldsymbol{l}$ be total angular momentum, silicon spin, carbon spin, channel spin, and orbital angular momentum, respectively. Let m_J, m_{Si}, m_{C}, m_S, and m_l be their respective magnetic substates with respect to the normal to the scattering plane. Although the compound nucleus will be formed with a broad spin distribution, the contribution to the carbon yield comes from a few partial waves near the critical angular momentum ($J_{\mathrm{crit}}=23\hbar$ at $E_{\mathrm{c.m.}}=43.5$ MeV, $J_{\mathrm{crit}}=25\hbar$ at $E_{\mathrm{c.m.}}=48$ MeV). We obtain the following expression for the density matrix using the Hauser-Feshbach formalism[19] for a specific value of J and S_{Si}. When the carbon particle is detected at an angle $\theta_{\mathrm{c.m.}}$ with respect to the beam axis, then the elements of the density matrix for the ^{12}C(2^+) state in a coordinate frame whose Z axis is normal to the scattering plane and X axis along the beam direction is given by

$$\rho m_c m_{c'} = \sum_S \sum_l \sum_{m_{\mathrm{Si}}} \sum_{m_J} \sum_{m_{J'}} \langle S_{\mathrm{C}}, S_{\mathrm{Si}}, m_{\mathrm{C}}, m_{\mathrm{Si}} | S, m_S \rangle \langle S, l, m_s, m_l | J, m_J \rangle$$
$$\times \langle S_{\mathrm{Si}} S_{\mathrm{C}}, m_{\mathrm{Si}}, m_{c'} | S, m_{s'}, m_{l'} | J, m_{J'} \rangle T_l(\varepsilon) \exp\{2[a(E_{\mathrm{c.m.}} - V_C - E_{\mathrm{rot}}]^{1/2}\}$$
$$\times Y_{l,m_l}\left[\frac{\pi}{2}, \theta_{\mathrm{c.m.}}\right] Y^*_{l,m_{l'}}\left[\frac{\pi}{2}, \theta_{\mathrm{c.m.}}\right] Y_{J,m_J}\left[\frac{\pi}{2}, 0\right] Y_{J,m_{J'}}\left[\frac{\pi}{2}, 0\right] . \quad (3)$$

Here a is the level density parameter, V_{C} is the Coulomb barrier, $E_{\mathrm{c.m.}}$ is the incident center-of-mass energy, and E_{rot} is the total rotational energy. T_l is the transmission coefficient of ^{12}C for orbital angular momentum l and exit channel kinetic energy ε. We obtained values of T_l by using an optical model potential.[20] The normalization was obtained by multiplying the calculated density matrix by $(\mathrm{tr}\rho)^{-1}$. A similar expression was used for ^{28}Si states also. The two curves in Fig. 11 were calculated for $J=21\hbar$, $23\hbar$, and $S_{\mathrm{Si}}=8\hbar$ for ^{12}C and $S_{\mathrm{Si}}=6\hbar$ for ^{28}Si. In Fig. 12, we show calculations for $J=23\hbar$, $25\hbar$, and $S_{\mathrm{Si}}=8\hbar$ for ^{12}C and $J=21\hbar$, $23\hbar$, and $S_{\mathrm{Si}}=6\hbar$ for ^{28}Si at $E_{\mathrm{c.m.}}=48$ MeV. The total rotational energy for E_{rot} was calculated by assuming a prolate ellipsoidal shape[21] for the excited ^{28}Si and a spherical ^{12}C nucleus touching each other, so that the major axis of ^{28}Si is along the line joining the centers of two nuclei. The statistical model code CASCADE[18] predicts that most of the contributions to the carbon yield come from $J>23\hbar$ at $E_{\mathrm{c.m.}}=43.5$ MeV and $J>25\hbar$ for $E_{\mathrm{c.m.}}=48$ MeV. So a weighted average over different values of J will significantly increase P_{zz} and worsen the already poor agreement with the experimental data. A weighted average over the distribution of S_{Si} obtained from CASCADE code calculations increases P_{zz} by approximately 10%.

We conclude that the statistical model calculation predicts much higher alignment than observed. Variation of the level density parameter and the shape of the nuclei within reasonable limits do not change this conclusion. In Fig. 13, the solid lines show the predictions of statistical model calculations for P_{zz} of the ^{12}C(2^+) state for $J=23\hbar$, $21\hbar$, and $S_{\mathrm{Si}}=8\hbar$ at $E_{\mathrm{c.m.}}=43.5$ MeV. We also show statistical model calculations for $J=23\hbar$, $25\hbar$, and $S_{\mathrm{Si}}=8\hbar$ at $E_{\mathrm{c.m.}}=48$ MeV. Again we find large discrepancies between statistical model calculations and observations.

The discrepancies with the statistical model extend also to off-diagonal elements of the density matrix. Using Eq. (3), we find that the statistical model predicts that the density matrix will be almost diagonal with respect to the normal to the reaction plane. To compare with the experimental results, we rotate the calculated density matrix to a coordinate frame where Z_{C} is the Z axis and the Y axis is normal to the reaction plane. The rotated density matrix has significant off-diagonal terms (ρ_{02},ρ_{1-1}) as shown in the third column of Table I, in disagreement with our observations. The calculations shown in Table I have been performed for $J=23\hbar$. We also find large off-diagonal elements $\rho_{02}=-0.068$, $\rho_{1-1}=-0.085$ for the ^{12}C(2^+) state even for $J=21\hbar$. Table III shows the calculated ratios of ^{12}C(2^+) to ^{12}C(g.s.) integrated over $Q<-10$ and $Q<-16$ MeV. We find that the statistical model predicts considerably larger ratios than observed.

Recent measurements by Sanders *et al.*[22] have also shown no evidence of any strong spin alignment of the ^{12}C fragments in ^{24}Mg(^{32}S, ^{12}C)^{44}Ti fully damped reaction. Although the authors claim that the absence of spin alignment implies statistical equilibrium, we find that large spin alignment can occur in statistical model calculations. The spin alignment parameter depends on the angle of emission of ^{12}C and its value drops sharply near the beam axis, independent of the reaction mechanism, because the values of spherical harmonics become smaller near the beam axis. In Ref. 22, most of the alignment data came from the measurements done at small angles.[23] So the absence of the spin alignment of the ^{12}C(2^+) state in the ^{32}S+^{24}Mg system does not necessarily imply statistical equilibration.

B. Sticking model.

The simple dinuclear sticking model[1,11] predicts that the spin alignment parameter P_{zz} (Z axis normal to the reaction plane) is equal to unity, independent of angle. The sticking model also predicts[11] that $^{12}C(2^+)$ state should be almost always excited. These predictions disagree with our observations.

C. Dinuclear orbiting model

Let us consider a simple picture of two nuclei connected by a narrow neck living long compared to the damping time of their relative motion. The twisting motion[24] between them will be small compared to bending[24] and wriggling[24] modes because of the assumption of a narrow neck.[25] If we assume that bending and wriggling modes dominate because of the structure of the orbiting complex and sum incoherently over different orientations of the spin angular momentum vectors lying randomly in a plane perpendicular to the body-fixed symmetry axis, then the density matrix of $^{12}C(2^+)$ with respect to the body-fixed symmetry axis is given by

$$\rho_{00}=0.375,\quad \rho_{11}=\rho_{-1-1}=0.25\ ,$$
$$\rho_{22}=\rho_{-2-2}=0.0625\ , \tag{4}$$
$$\rho_{01}=\rho_{02}=\rho_{12}=\rho_{1-1}=\rho_{2-2}=\rho_{1}-2=0\ .$$

In the body-fixed frame, the dinuclear system breaks along the symmetry axis. Here the Coulomb energy $V_C=18.1$ MeV and orbital energy $V_l=l(l+1)/2I_R=6.2$ MeV for $l=12\hbar$, where I_R is the moment of inertia of the relative motion. So in a space-fixed frame, the trajectory of emitted ^{12}C will be rotated by $\pm\tan^{-1}(V_l/V_C)^{0.5}=\pm30°$ with respect to the body-fixed symmetry axis. We rotate the density matrix Eq. (4) by $\pm30°$ and take an average. The results, shown in the last column of Table I, are in better agreement with the experimental data than are the statistical model calculations as shown by the small off-diagonal (ρ_{02},ρ_{1-1}) elements. A similar analysis for the ^{28}Si state also predicts approximate symmetry of ^{28}Si states with respect to the direction of motion of ^{28}Si. We also obtain alignment parameters of 0.24 and 0.25 (as shown by dashed line in Figs. 11 and 12), with respect to the normal to the reaction plane for $^{12}C(2^+)$ and ^{28}Si states, in agreement with our observation.

Our simple classical dinuclear model does not predict any variation of alignment parameter and density matrix with the angle of emission of carbon particles. This model is not quantitatively valid near $\theta_{c.m.}=180°$, where we expect significant variation of alignment parameter and elements of density matrix with the angle of emission of carbon particles. However, this model qualitatively agrees with the observed γ-ray angular correlation at $\theta_{c.m.}=180°$ because, according to this model, the spin angular momentum vectors will lie in a plane perpendicular to the beam axis when ^{12}C is detected at $\theta_{c.m.}=180°$, in agreement with observation.[11] Table II shows that in the more inelastic Q-value bin $-40<Q<-22$ MeV, the measured value of ρ_{22} along the direction of motion is larger than expected from dinuclear orbiting model calculations. As a result, we see in Fig. 13 that P_{zz} is smaller (0.1 ± 0.05) than expected from the dinuclear orbiting calculation, as shown by dashed lines. This can be understood because the angular momentum misalignment along the body-fixed symmetry axis (twisting mode) increases as the Q value decreases and therefore ρ_{22} along the direction of motion increases and the alignment parameter is reduced. Also, some of the excited carbon particles in this bin can come from ^{16}O and so will be less aligned.

Table III shows the disagreement between the calculated ratios from statistical model and measured ratios of yields of the $^{12}C(2^+)$ to ^{12}C(g.s.). The lower values of $^{12}C(2^+)/^{12}C$(g.s.) qualitatively supports the dinuclear orbiting picture, where the nonexcitation of the twisting mode will lower the ratio compared to statistical model calculations.

D. Application of orbiting model to other observables

Let us consider the consequences of our modified orbiting picture on the observables other than γ-ray angular correlation.

1. *Angular distribution*

If τ is the mean lifetime and ω the angular velocity of the dinuclear system, then the angular distribution of a decaying product from such a system is given by[26]

$$\frac{d\sigma}{d\omega}=\frac{\text{const}}{\sin\theta}\{\exp(-\theta/\omega\tau)+\exp[-(2\pi-\theta)/\omega\tau]\}\ .$$

We see from the above equation that if $\tau\gg2\pi/\omega$, the angular distribution has the form $1/\sin\theta$. This result is not affected by the assumption of a narrow neck between the two nuclei.

2. *Large yield and entrance-channel effect*

The large yields of carbon and oxygen particles from the $^{28}Si + {}^{12}C$ reaction has been explained before by using the equilibrated orbiting model.[4] This model is a constrained phase-space model with the dinuclear sticking-model configuration. We find from the present work that this configuration should be replaced by a dinuclear configuration in which the two nuclei are connected by a narrow neck undergoing mainly orbiting, bending and wriggling motions. Qualitatively speaking, the observed large yields and entrance-channel effects are natural consequences of the assumed dinuclear configuration connected by a narrow neck in which the shape degree of freedom does not equilibrate. However we still do not have a quantitative model to understand the large yields and entrance-channel effects in some systems[9,5] and the lack of those effects in other systems.[6,7]

3. *Selective population of natural parity states*

The observed selective population of natural parity states in the $^{24}Mg + {}^{12}C$ reaction[10] also supports the dinuclear reaction mechanism. In compound nucleus reac-

tions, both natural and unnatural parity transitions are allowed. Orbiting is probably a multistep direct-reaction process. Austern and Blair[27] have shown that in the multistep direct-reaction processes involving projectiles with zero-spin, final states having only natural parities are selected if the following conditions are satisfied.

(a) The collective coordinates of the system vary very slowly in the intermediate states so that the transition amplitude from the initial nuclear state to the final nuclear state does not depend explicitly on the collective coordinates of the system. As a result the relevant Green's function is independent of the nuclear Hamiltonian involving collective coordinates of the system.

(b) The displacement operator of collective deformations of the nuclear surface commutes with the Green's function so that the interactions can be combined to give only one spherical harmonic of a single argument. Austern and Blair[27] have shown that this is a reasonable assumption for strongly absorbed projectiles which have short wavelength.

If we consider the formation of a long-lived dinuclear intermediate state where the two nuclei are connected by a narrow neck, then the collective coordinates should vary slowly and the above conditions are satisfied approximately.

V. CONCLUSION

We have made the first measurements of density matrices of ^{12}C and ^{28}Si states produced in the $^{28}Si + {}^{12}C$ reaction and found that the density matrices are diagonal with respect to their directions of motion. The determination of the complete density matrix is the most powerful and completely model-independent way to determine the symmetry axis of the spin distribution. A Hauser-Feshbach calculation fails to account for the data. Our observation is consistent with the picture of a long-lived dinuclear system connected by such a narrow neck that orbiting, bending, and wriggling motions are the dominant spin carrying modes. The γ-ray angular correlation observed when ^{12}C is detected at backward angles is consistent with this dinuclear orbiting picture. Both the Hauser-Feshbach calculation and the equilibrated orbiting model predict a large alignment parameter normal to the reaction plane and approximate cylindrical symmetry of the spin angular momentum vectors with respect to the normal to the reaction plane, in disagreement with observations. However, it cannot be ruled out that the observations of large yields, entrance-channel effect, selective population of natural parity states, γ-ray angular correlation at $\theta_{c.m.} = 180°$ and the observed spin alignment parameters and density matrices distribution may result from the complicated dynamical processes of fusion and fission of the compound nucleus. Ritzka *et al.*[28] have shown from the measurement of in-plane angular distribution that for $^{20}Ne + {}^{168}Er$ system at $E_{c.m.} = 241.3$ MeV, the spin distribution is symmetric with respect to the exit-channel orbital angular momentum for deep inelastic region. We think that the reaction mechanism and symmetry of the spin distribution changes for heavier systems and at higher bombarding energy may come closer to the predictions of a compound nuclear reaction mechanism.

In conclusion, the present modified orbiting model is in qualitative agreement with all observations performed on similar systems. The concept of orbiting is a classical macroscopic concept. We have not yet understood orbiting from a more fundamental point of view. In principle, one should do coupled-channel and time-dependent Hartree-Fock calculations to find out how far the classical concept of orbiting can be supported. However in this large Q-value region, where almost a continuum of states is contributing, it has not been possible to perform any such calculations. Sanders *et al.*[29] explained the backward-angle yields of the ^{24}Mg (^{16}O ,^{12}C)^{28} Si(g.s.) and ^{24}Mg (^{16}O ,^{12}C) $^{28}Si(2^+)$ reactions by putting in resonances in distorted-wave Born approximation calculations and discussed their observations in terms of nuclear molecular resonances. We think that nuclear molecular resonances are responsible for the large back angle yields of highly excited states also. However, in large Q-value regions, it becomes increasingly more difficult to perform such resonance analysis. So for the purpose of studying the gross features of the reactions integrated over large Q-value bins, we consider it justified to try to understand the reaction mechanism by using the classical orbiting picture rather than using nuclear molecular resonance description. Such a picture has its limitations, but at present we at least have a qualitative understanding of the reaction mechanism.

ACKNOWLEDGMENTS

We thank the staff of HHIRF and acknowledge useful discussions with Dr. D. C. Hensley (ORNL), Dr. G. R. Satchler (ORNL), Dr. J. Wu (JIHIR), Dr. S. Ayik (Tennessee Technological University), Dr. R. Vandenbosch (University of Washington) and Dr. R. P. Schmitt (Texas A&M University). This work was supported by the U. S. Department of Energy under Contract Nos. DE-FG05-87ER40361 with the University of Tennessee, DE-AC05-840R21400 with Martin Marietta Energy Systems, Inc., and DE-AC02-ER03074 with Yale University.

[1]D. Shapira, R. Novotny, Y. D. Chan, K. A. Erb, J. L. C. Ford, Jr., J. C. Peng, and J. D. Moses, Phys. Lett. **114B**, 111 (1982).

[2]D. Shapira, J. L. C. Ford, Jr., and J. Gomez del Campo, Phys. Rev. C **26**, 2470 (1982).

[3]D. Shapira, J. L. C. Ford, Jr., J. Gomez del Campo, and P. H. Stelson, Phys. Rev. C **21**, 1824 (1980).

[4]B. Shivakumar, S. Ayik, B. A. Harmon, and D. Shapira, Phys. Rev. C **35**, 1730 (1987).

[5]S. Ayik, D. Shapira, and B. Shivakumar, Phys. Rev. C **38**, 2610 (1988).

[6]S. Sanders, D. G. Kovar, B. B. Back, C. Beck, B. K. Ditcher, D. Henderson, R. V. F. Janssens, J. G. Keller, S. Kaufman,

T. F. Wang, B. Wilkins, and F. Videbaek, Phys. Rev. Lett. **59**, 2856 (1987).
[7]C. Beck, B. Djerroud, B. Heusch, R. Dayras, R. M. Freeman, F. Haas, A. Hachem, J. P. Wieleczko, and M. Youlal, Z. Phys. A **334**, 521 (1989).
[8]D. Shapira, Phys. Rev. Lett. **61**, 2153 (1988).
[9]A. Ray, S. Gil, M. Khandaker, D. D. Leach, D. K. Lock, and R. Vandenbosch, Phys. Rev. C **31**, 1573 (1985).
[10]W. Dunnweber, A. Glaesner, W. Hering, R. Ritzka, W. Trombik, J. Czakanski, and W. Zipper, Phys. Rev. Lett. **61**, 927 (1988).
[11]A. Ray, D. D. Leach, R. Vandenbosch, K. T. Lesko, and D. Shapira, Phys. Rev. Lett. **57**, 815 (1986).
[12]M. Jaaskelainen, D. G. Sarantites, R. Woodward, F. A. Dilmanian, J. T. Hood, R. Jaaskelainen, D. C. Hensley, M. L. Halbert, and J. H. Barker, Nucl. Instrum. Methods **204**, 385 (1983).
[13]P. Dyer, D. Bodansky, A. G. Seamster, E. B. Norman, and D. R. Maxson, Phys. Rev. C **23**, 1865 (1981).
[14]G. R. Satchler, *Direct Nuclear Reactions* (Oxford University Press, England, 1983).
[15]H. J. Rose and D. M. Brink, Rev. Mod. Phys. **39**, 306 (1967).
[16]Z. Berant, M. B. Goldberg, G. Goldring, S. S. Hanna, H. M. Loebenstein, I. Plesser, M. Popp, J. S. Sokolowski, P. N. Tandon, and Y. Wolfson, Nucl. Phys. **A178**, 155 (1971).
[17]T. Dossing, Nucl. Phys. **A357**, 488 (1981).
[18]F. Puhlhofer, Nucl. Phys. **A280**, 267 (1977).
[19]H. Feshback, in *Nuclear Spectroscopy,* edited by F. Ajzenberg-Selove (Academic, New York, 1960), Part B.
[20]C. M. Perey and F. G. Perey, At. Data Nucl. Data Tables **17**, 1 (1976).
[21]F. Glatz, P. Betz, J. Siefert, F. Heidinger, and H. Ropke, Phys. Rev. Lett. **46**, 1559 (1981).
[22]S. J. Sanders, B. B. Back, R. V. F. Janssens, D. G. Kovar, D. Habs, D. Henderson, T. L. Khoo, H. Korner, G. E. Rathke, T. F. Wang, F. L. H. Wolfs, and K. B. Beard, Phys. Rev. C **41**, 1901 (1990).
[23]S. J. Sanders, private communication.
[24]R. P. Schmitt and A. J. Pacheco, Nucl. Phys. **A379**, 313 (1982).
[25]R. Vandenbosch, Phys. Rev. C **20**, 171 (1979).
[26]T. Mikumo, M. Sasagase, M. Sato, T. Ooi, Y. Higashi, Y. Nagashima, and M. Yamanouchi, Phys. Rev. C **21**, 620 (1980).
[27]N. Austern and J. S. Blair, Ann. Phys. (N.Y.) **33**, 15 (1965).
[28]R. Ritzka, W. Dunnweber, A. Glaesner, W. Hering, W. Trombik, A. Budzanowski, M. Burgel, and H. Homeyer, Phys. Lett. B **200**, 8 (1988).
[29]S. J. Sanders, H. Ernst, W. Henning, C. Jachcinski, D. G. Kovar, J. P. Schiffer, and J. Barrette, Phys. Rev. C **31**, 1775 (1985).